Dopamine-dependent synaptic plasticity in striatum during *in vivo* development

Ka-Choi Tang*, Malcolm J. Low†, David K. Grandy‡, and David M. Lovinger*§

*Department of Molecular Physiology and Biophysics and Center for Molecular Neuroscience, Vanderbilt University Medical School, Nashville, TN 37232-0615; and †Vollum Institute and ‡Department of Physiology and Pharmacology, Oregon Health Sciences University, Portland, OR 97201

Edited by P. S. Goldman-Rakic, Yale University School of Medicine, New Haven, CT, and approved November 10, 2000 (received for review August 8, 2000)

The neurotransmitters dopamine (DA) and glutamate in the striatum play key roles in movement and cognition, and they are implicated in disorders of the basal ganglia such as Parkinson's disease. Excitatory synapses in striatum undergo a form of developmental plasticity characterized by a decrease in glutamate release probability. Here we demonstrate that this form of synaptic plasticity is DA and DA D2 receptor dependent. Analysis of spontaneous synaptic responses indicates that a presynaptic mechanism involving inhibition of neurotransmitter release underlies the developmental plasticity. We suggest that a major role of DA in the striatum is to initiate mechanisms that regulate the efficacy of excitatory striatal synapses, producing a decrease in glutamate release.

The striatum is the point of entry of information into the basal ganglia, and it has important roles in motor control and habit learning (1, 2). The neocortex (3, 4) and thalamus (5) provide the major excitatory inputs to striatal medium spiny projection neurons (MSNs). Morphological studies have demonstrated that the majority of these afferent terminals impinge on the head of the spines on the dendrites of striatal MSNs (6, 7), whereas most dopaminergic afferent fibers coming from the substantia nigra make synapses on the necks of the same dendritic spines (8). This close anatomical localization of these two types of synapses suggests that dopamine (DA) released from the nigrostriatal afferent terminals may have modulatory effects on the excitatory signals generated from the cortex and thalamus (9).

The importance of DA in normal striatal function is evidenced by the severe disruption of behavior observed in Parkinson's disease and after chemical lesions of nigral dopaminergic inputs to striatum (10). In fact, DA plays a variety of important physiological roles in striatum (11–15). However, the cellular physiological actions of DA that contribute to striatal function *in vivo* are not fully understood. In the present study, we wanted to examine the role of the DA system in plasticity of synaptic efficacy at striatal glutamatergic synapses during early postnatal development.

Long-term changes in synaptic efficacy have been postulated to be cellular mechanisms underlying learning and memory (16). Synaptic plasticity of this type may also be involved in maturation of central synapses. One form of synaptic plasticity that may play an important role in maturation of excitatory synapses in the striatum is a decrease in the efficacy of transmission that takes place during weeks 2–3 of postnatal development (17, 18). This decrease in efficacy appears to involve a decrease in glutamate release. However, little is known about the role of different striatal neurotransmitters in this developmental plasticity.

To determine whether DA plays a role in the synaptic plasticity during maturation of excitatory striatal synapses we examined synaptic transmission at glutamatergic synapses in two animal models over the period from postnatal day (PD) 12 to PD29. One model was a unilateral intrastriatal 6-hydroxydopamine (6-OHDA) lesions in rats. The second model was the DA D2 receptor knockout (D2KO) mouse developed by Low and colleagues (19). To estimate changes in relative release probability, we measured the paired-pulse ratio (PPR) at excitatory striatal synapses in brain slices by using whole cell recording. PPR is a well-accepted measure of the probability of neurotransmitter release at presynaptic terminals (20). An increase in this measure is usually indicative of a decrease in the probability of release (21).

The present study provides evidence that the decrease in glutamate release probability observed during *in vivo* striatal development is DA and DA D2 receptor-dependent. We also provide evidence that this process involves inhibition of release independent of neuronal excitability. These findings present compelling evidence that this change in synaptic efficacy occurs naturally *in vivo* and is dependent on the actions of a neurotransmitter, namely DA, that has crucial roles in striatal function.

Materials and Methods

Intrastriatal 6-OHDA Injection. After rats (PD7) were anesthetized with methoxyflurane, they were fixed in a homemade mold on a stereotaxic instrument. An incision was made in the skin on the head by using a scalpel to expose the skull. A small hole was drilled in the skull at coordinates AP 0.1 mm anterior to bregma, L 2.0 mm from the midline. A 15-μg dose of 6-OHDA (Sigma) dissolved in 1 μl of saline with 0.1% ascorbic acid was intrastriatally injected at a depth of 4.0 mm below the skull. Control rats were injected with 1 μl of saline at the same coordinates. One week or more later, rats were killed for electrophysiological studies. Animal care in all experiments was in accordance with institutional guidelines.

Brain Slice Preparation. Brain slices were prepared from PD12–29 animals. Pregnant Sprague–Dawley rats were obtained from Sasco (Omaha, NE). The wild-type (WT) mice used were C57BL/6J mice purchased from The Jackson Laboratory or N10 congenic C57BL/6J mice bred at the Oregon Health Sciences University. The congenic mice were backcrossed for 10 generations onto the C57BL/6J genetic background, and N10 breeding pairs of homozygous *Drd2* +/+ or −/− mice were used to generate the pups for these studies. Data from the two sets of WT mice were pooled because there was no difference between mice from the two sources. Animals were killed by decapitation, and the brains were quickly removed and placed in an ice-cold, modified artificial cerebrospinal fluid (aCSF) containing (in mM): 194 sucrose, 30 NaCl, 4.5 KCl, 1 $MgCl_2$, 26 $NaHCO_3$, 1.2

This paper was submitted directly (Track II) to the PNAS office.

Abbreviations: MSNs, medium spiny projection neurons; DA, dopamine; 6-OHDA, 6-hydroxydopamine; D2KO, DA D2 receptor knockout; PD*n*, postnatal day *n*; PPR, paired-pulse ratio; WT, wild type; EPSC, excitatory postsynaptic current; sEPSC, spontaneous EPSC; mEPSC, miniature EPSC; HFS, high-frequency stimulation; LTD, long-term depression; TH, tyrosine hydroxylase; VEH, vehicle; TTX, tetrodotoxin.

§To whom reprint requests should be addressed at: Vanderbilt University Medical School, Department of Molecular Physiology and Biophysics, Room 724, Medical Research Building 1, Nashville, TN 37232-0615. E-mail: david.lovinger@mcmail.vanderbilt.edu.

The publication costs of this article were defrayed in part by page charge payment. This article must therefore be hereby marked "*advertisement*" in accordance with 18 U.S.C. §1734 solely to indicate this fact.

Article published online before print: *Proc. Natl. Acad. Sci. USA*, 10.1073/pnas.031374698. Article and publication date are at www.pnas.org/cgi/doi/10.1073/pnas.031374698

NaH_2PO_4, and 10 D-glucose. Modified aCSF was adjusted to pH 7.4 by bubbling with 95% O_2/5% CO_2. Coronal sections (400 μm thick) were cut in ice-cold modified aCSF by using a manual Vibroslice (Campden Instrument, Sileby, Loughborough, U.K.). Slices were then transferred to a nylon net submerged in normal aCSF containing (in mM): 124 NaCl, 4.5 KCl, 2 $CaCl_2$, 1 $MgCl_2$, 26 $NaHCO_3$, 1.2 NaH_2PO_4, and 10 D-glucose. Normal aCSF was oxygenated and maintained at pH 7.4 by bubbling with 95% O_2/5% CO_2 at room temperature (22–24°C). After incubation for 1 hr, a hemislice containing the cortex and striatum at the level of the head of the caudate was completely submerged in a Plexiglas recording chamber and continuously superfused with normal aCSF at a flow rate of 2–3 ml/min. Normal aCSF or drugs in aCSF were delivered to the recording chamber by superfusion driven by gravity flow. The temperature of the bath solution was kept at 32–35°C and was stable within ±1°C in a given experiment.

Whole-Cell Voltage-Clamp Recordings. Stimulus-evoked excitatory postsynaptic currents (EPSCs) in the lateral portion of the dorsal striatum were recorded using an Axopatch 1-D amplifier. Pipettes had resistances of 3–5 MΩ when filled with an internal solution containing (in mM): 120 $CsMeSO_3$, 5 NaCl, 10 tetraethylammonium chloride, 10 Hepes, 3–5 QX-314 (lidocaine *N*-ethyl bromide), 1.1 EGTA, 4 ATP (Mg^{2+} salt), and 0.3 GTP (Na^+ salt), pH adjusted to 7.2 with CsOH, osmolarity adjusted to 270–280 mOsm with sucrose. A small number of recordings were made with an internal solution containing (in mM): 130 $KMeSO_4$, 1 $MgCl_2$, 0.1 $CaCl_2$, 10 Hepes, 1 EGTA, 2 ATP (Mg^{2+} salt), and 0.4 ATP (Na^+ salt), pH adjusted to 7.2 with KOH. Recordings from MSNs within three or four cell diameters below the surface of slices were made under differential interference contrast (DIC)-enhanced visual guidance. Neurons were voltage-clamped at −70 mV during recording periods before and after application of high-frequency stimulation (HFS). Stimuli were delivered every 20 s through bipolar twisted tungsten electrodes placed in the white matter dorsal to the striatum. The series resistance, which was not compensated and was typically between 5 and 10 MΩ, was monitored continuously. Once a stable recording with an EPSC of ≈200 pA amplitude triggered by 0.05-Hz stimuli had been maintained at least for 5 min, long-term depression (LTD) was induced by pairing HFS, consisting of four 100-Hz trains of 1-s duration delivered at a frequency of one train every 10 s, with simultaneous 1-s depolarizations of the postsynaptic neuron to −10 mV. Signals were filtered at 5 kHz, digitized at ≤20 kHz with a DigiData 1200, and stored on a Dell Dimension Pentium microcomputer using commercially available software (pCLAMP6).

The EPSC amplitudes were analyzed by using peak detection software provided in pCLAMP6. The representative EPSC waveforms shown in the figures are the average of 10–15 individual responses in a given recording. Paired-pulse responses were elicited by paired stimuli with an interstimulus interval of 50 ms. PPR was calculated as the ratio of the amplitude of the second EPSC to that of the first EPSC. All values are averaged from data obtained over 5–10 min and presented as mean ± SE. Spontaneous EPSCs (sEPSCs) and miniature EPSCs (mEPSCs) were stored on videotape digitized onto a Pentium microcomputer and analyzed by using MINI ANALYSIS program (Version 4.3; Synaptosoft, Leonia, NJ). The threshold for detection of the events was the baseline rms noise level (range 2.5–5.4 pA) for each cell (measured with the MINI ANALYSIS software). Number of events per unit time, peak amplitude, rise time, and decay time constant were measured. Rise time (10–90%) is the time taken to rise from 10% to 90% of the peak amplitude in the initial phase of the response. Decay time constant is the time to decay from 90% to 37% of peak amplitude on the falling phase of the response. Input resistance was determined by measuring the steady-state current response to 5-mV pulses under voltage-clamp. Data were analyzed with a two-tailed Student's *t* test and two- or one-way ANOVA. The statistical criterion for significance was $P < 0.05$.

Tyrosine Hydroxylase (TH) Immunocytochemical Staining. After overnight fixation in 4% paraformaldehyde, slices were placed into 0.1 M sodium phosphate (pH 7.4) or into a cryoprotectant solution (30% sucrose and 30% ethylene glycol in 0.1 M sodium phosphate, pH 7.4) for storage at −20°C. Coronal sections were cut through the slice at 40 μm. Sections were then washed in 50 mM Tris-buffered saline (TBS; pH 7.4) and incubated in TBS containing 4% normal horse serum and 0.2% Triton X-100 (TBS+) for 20 min. Sections were incubated in the mouse anti-TH primary antibody (1:3000) in TBS+ for 24–48 hr at 4°C. The sections were then washed in TBS+, incubated in a biotinylated donkey anti-mouse secondary antibody (1:2000) in TBS+ for 90 min, washed in plain TBS, and then placed in peroxidase-coupled streptavidin (1:200) for 60 min. After sections were washed in TBS, TH immunoreactivity was revealed by incubation in 3,3-diaminobenzidine and 0.03% hydrogen peroxide in TBS.

Results

DA-Dependent Decreases in Presynaptic Release Probability in Striatum. In rats given intrastriatal injections of saline vehicle (VEH) at PD7, there was a developmental increase in PPR (Fig. 1*A* and *B*) similar to our previous observations in untreated rats (18). The shift to greater PPR values was most prominent around PD20–21 (Fig. 1*B*). However, no developmental PPR change was observed in rats with 6-OHDA lesions (Fig. 1*B*). Fig. 1*C* shows that there is a severe loss of TH immunoreactivity in the 6-OHDA-lesion side of the dorsolateral striatum in the region where recordings were performed. Similar results were observed in naïve WT and D2KO mice, with the PPR increasing over development in WT but not in D2KO mice (Fig. 1 *D* and *E*). These data strongly suggest that DA and activation of D2 receptors are important in determining the pattern of change in release probability during early postnatal development.

We also measured PPR in a small number of neurons from young and old untreated rat striatum with a K^+-based internal solution. The average PPR from PD12–13 rats was 0.85 ± 0.03 ($n = 4$), whereas the average PPR from a PD26 rat was 1.23 ($n = 2$). These data suggest that the developmental change in probability of release can be observed when recordings are made in the presence of intracellular K^+.

DA-Dependent Developmental Changes in mEPSC Frequency. We also observed a significant developmental decrease in the frequency of sEPSCs in untreated rats (Fig. 2*A*) and WT mice (Fig. 2*B*), consistent with the idea that synaptic plasticity involving a decrease in glutamate release takes place *in vivo* at striatal synapses during postnatal development. This developmental decrease in the frequency of sEPSCs was not observed in rats with 6-OHDA lesions (Fig. 3*A*) and D2KO mice (Fig. 3*D*). In fact, the frequency of sEPSCs observed in PD21–27 DA-depleted and D2KO animals was similar to that observed in younger control animals. Thus, the frequency of sEPSCs was significantly higher in >PD20 6-OHDA-treated (Fig. 3*C*) and D2KO (Fig. 3*F*) animals than in >PD20 VEH-treated rat and WT mouse striatum, respectively.

A similar high frequency of sEPSCs was also observed in the presence of a voltage-sensitive sodium channel blocker, tetrodotoxin (TTX; 100 nM; Alomone Labs, Jerusalem) (Fig. 3 *B* and *C*, data for 6-OHDA-treated rats; Fig. 3 *E* and *F*, data for D2KO mice), suggesting that the recorded sEPSCs were action potential-independent mEPSCs, as we have previously demonstrated in untreated rats (22). These mEPSCs represent glutamate

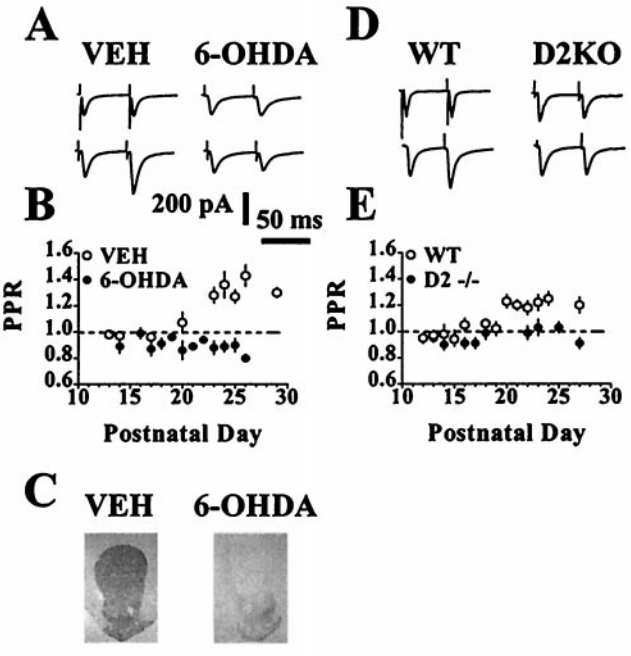

Fig. 1. Loss of the developmental increases in PPR in intrastriatal 6-OHDA-treated rats and D2KO mice. (*A*) The left traces are EPSCs elicited by paired stimuli (50-ms interpulse interval) recorded in neurons from different aged VEH-treated rats (upper traces, PD13; lower traces, PD26). The right traces are EPSCs recorded in neurons from different aged 6-OHDA-treated rats (upper traces, PD16; lower traces, PD26). (*B*) Summary plot of PPR across the early postnatal developmental period. Data obtained from VEH- (40 neurons in 19 rats) and 6-OHDA- (74 neurons in 28 rats) treated animals are expressed as open and solid circles, respectively. Number of cells recorded in VEH-treated rats at different ages was 4 at PD13, 5 at PD14, 3 at PD17, 8 at PD20, 5 at PD23, 4 at PD24, 4 at PD 25, 3 at PD26, and 4 at PD29. Number of cells recorded in 6-OHDA-treated rats at different ages was 4 at PD14, 3 at PD16, 4 at PD17, 4 at PD18, 7 at PD19, 7 at PD20, 5 at PD 21, 8 at PD22, 8 at PD23, 12 at PD24, 8 at PD25, and 4 at PD26. Two-way ANOVA analysis showed that PPR was significantly different between 6-OHDA-treated and VEH-treated rats ($F = 65.6$, df = 1/65, $P < 0.0001$) and dependent upon age ($F = 2.79$, df = 6/65, $P < 0.05$). (*C*) The extent of DA denervation was examined by performing TH immunostaining on 40-μm-thick brain sections after electrophysiological experiments were completed. (*Left*) VEH injection. (*Right*) 6-OHDA injection. (*D*) Left traces are EPSCs recorded in neurons from different aged WT mice (upper traces, PD12; lower traces, PD24). The right traces are EPSCs recorded from different aged D2KO mice (upper traces, PD15; lower traces, PD25). (*E*) Summary plot of PPR across the early postnatal developmental period. Data obtained from WT (89 neurons in 30 mice) and D2KO (80 neurons in 28 mice) animals are expressed as open and solid circles, respectively. Number of cells recorded in WT mice was 6 at PD12, 8 at PD13, 3 at PD14, 8 at PD15, 3 at PD16, 6 at PD18, 10 at PD19, 4 at PD20, 4 at PD21, 13 at PD22, 15 at PD23, 4 at PD24, and 5 at PD27. Number of cells recorded in D2KO mice was 13 at PD13, 5 at PD14, 5 at PD15, 6 at PD16, 9 at PD17, 7 at PD18, 12 at PD22, 9 at PD23, 7 at PD25, and 7 at PD27. Two-way ANOVA analysis showed that PPR was significantly different between WT and D2KO mice ($F = 20.00$, df = 1/99, $P < 0.0001$) and dependent upon age ($F = 2.14$, df = 7/99, $P < 0.05$). Further analysis with one-way ANOVA indicated no significant change in PPR during postnatal development in 6-OHDA-treated rats ($F = 0.25$, df = 6/40, $P > 0.95$) and D2KO mice ($F = 0.83$, df = 7/52, $P > 0.84$). However, there was a significant increase in PPR during postnatal development in VEH-treated rats ($F = 3.35$, df = 6/25, $P < 0.05$) and WT mice ($F = 3.97$, df = 7/53, $P < 0.01$).

release events that occur independently of presynaptic action potentials and activation of voltage-gated Ca^{2+} channels (23). Thus, our findings suggest that the DA-dependent decrease in release may involve a change in vesicle-release-related mechanisms downstream from excitation/secretion coupling at the presynaptic terminal.

Removal of DA or D2 receptors might enhance synaptic

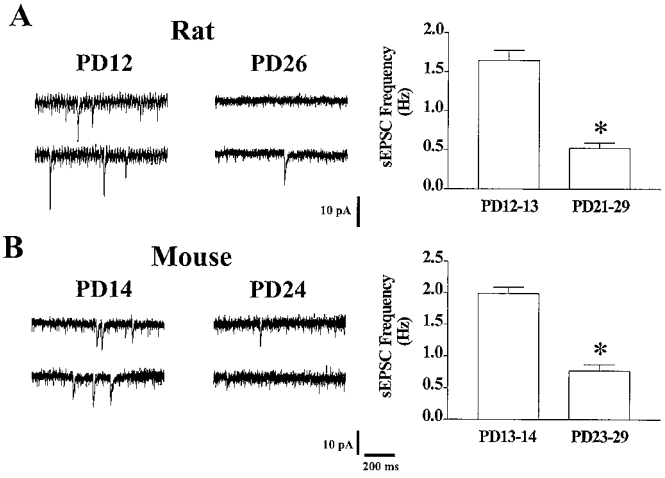

Fig. 2. A developmental decrease in basal frequency of spontaneous release occurs in intact animals. (*A*) (*Left*) Representative responses obtained from young (PD12) and mature (PD26) rats. (*Right*) Summary of basal frequency of sEPSCs in PD12–13 ($n = 5$) and PD21–29 ($n = 8$) rat neurons, (unpaired *t* test, $P < 0.0001$). (*B*) (*Left*) Representative responses obtained from young (PD14) and mature (PD24) mice. (*Right*) Summary of basal frequency of sEPSCs in PD13–14 ($n = 5$) and PD23–29 ($n = 7$) mouse neurons, (unpaired *t* test, $P < 0.0001$). Values are expressed as mean ± SE. Asterisks indicate statistically significant differences ($P < 0.05$) between young and mature groups.

transmission by removing tonic action of DA that requires constant activation of presynaptic D2 receptors. To assess this possibility, we applied a combination of D1 and D2 receptor antagonists (1 μM SKF-83566 and 1 μM sulpiride) during whole-cell recordings in >PD20 untreated rats. This treatment did not elicit an increase in sEPSC frequency (before antagonist treatment = 0.64 ± 0.12 Hz; after antagonist treatment = 0.59 ± 0.08 Hz, paired *t* test, $P > 0.9$, $n = 5$), a decrease in PPR (before antagonist treatment = 1.28 ± 0.1; after antagonist treatment = 1.24 ± 0.1, paired *t* test, $P > 0.2$, $n = 5$), or a change in EPSC amplitude (response after antagonist treatment averaged 99.8% ± 2.5% of control values, $n = 5$). Striatal LTD induced by HFS was blocked by this antagonist treatment. In three cells, when HFS was applied in the presence of D1 and D2 antagonists, LTD induction was prevented (EPSC amplitude at 20–30 min after HFS = 92.40% ± 2.7% of pre-HFS control, paired *t* test, $P > 0.2$), indicating that 1 μM concentrations of these antagonists prevented synaptic DA action in our brain slice preparation. Thus, the ineffectiveness of the antagonists in altering basal synaptic transmission is not due to a general lack of antagonist action in slices.

Lack of Involvement of Postsynaptic Mechanisms. The developmental decrease in sEPSC frequency observed in untreated rats or WT mice, and the high sEPSC frequency observed in 6-OHDA-injected rats or D2KO mice, do not appear to be due to changes in postsynaptic membrane properties that might affect the quantal amplitude and alter the detection of sEPSCs. We examined the amplitude of sEPSCs, distribution of sEPSC amplitudes, and the input resistance of recorded neurons obtained in both species under all experimental conditions. As shown in Fig. 4*A*, there is no significant age- or treatment-related difference in the average amplitude of sEPSCs observed in either species. Fig. 4*A Upper* shows that there is no significant difference in the average amplitude of sEPSCs obtained from young and mature rats that received different treatments. Fig. 4*A Lower* shows that there is no significant difference in the average amplitude of sEPSCs obtained from young WT, mature WT, and mature D2KO mice. To compare the distribution of sEPSC

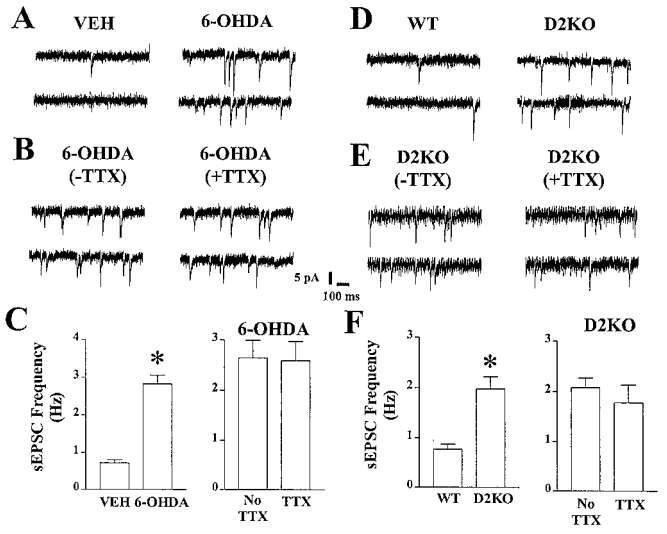

Fig. 3. Basal frequency of sEPSCs at striatal glutamatergic synapses remains high in mature 6-OHDA-treated rats and D2KO mice. (*A*) Representative recordings from VEH-treated (*Left,* PD25) and 6-OHDA-treated (*Right,* PD25) rat neurons. (*B*) Representative traces recorded in the absence (*Left*, PD24) and presence (*Right*, PD24) of 100 nM tetrodotoxin (TTX) in a 6-OHDA-treated rat neuron. (*C*) (*Left*) Summary of basal frequency of sEPSCs in neurons from VEH-treated (PD21–29; $n = 9$) and 6-OHDA-treated (PD21–26; $n = 13$) rats (unpaired t test, $P < 0.0001$). (*Right*) Summary of basal frequency of sEPSCs in the absence and presence of 100 nM TTX ($n = 6$) (paired t test, $P > 0.7$) in 6-OHDA-treated rat neurons. (*D*) Representative recordings from WT (*Left*, PD25) and D2KO (*Right*, PD25) mouse neurons. (*E*) Representative traces recorded in the absence (*Left*, PD25) and presence (*Right*, PD25) of 100 nM TTX in a D2KO mouse neuron. (*F*) (*Left*) Summary of basal frequency of sEPSCs in neurons from WT (PD21–27; $n = 7$) and D2KO (PD22–27; $n = 10$) mice (unpaired t test, $P = 0.001$). (*Right*) Summary of basal frequency of sEPSCs in the absence and presence of 100 nM TTX in neurons from D2KO mice ($n = 4$), (paired t test, $P > 0.2$). Values are expressed as mean ± SE. Asterisks indicate statistically significant differences ($P < 0.05$) between VEH- and 6-OHDA-injected rats or WT and D2KO mice.

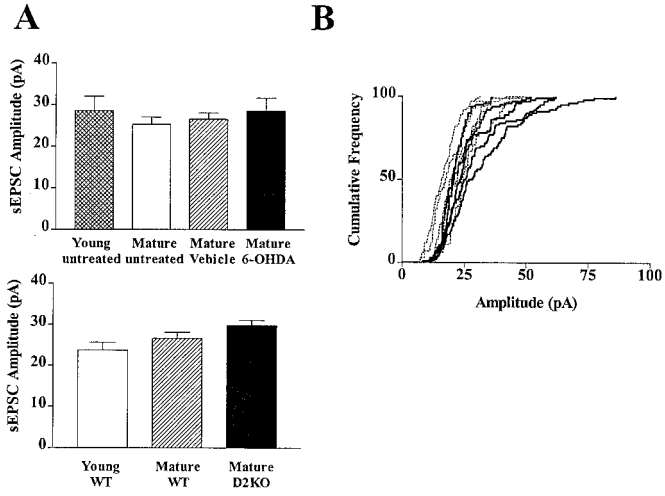

Fig. 4. (*A*) (*Upper*) Comparison of the average amplitude of sEPSCs recorded from striatal neurons obtained from different aged rats (untreated young, $n = 6$, vs. untreated mature, $n = 9$; unpaired t test, $P > 0.3$), and mature rats that received different treatments (VEH-treated, $n = 7$, vs. 6-OHDA-treated, $n = 7$; unpaired t test, $P > 0.5$). (*Lower*) Comparison of the average amplitude of sEPSCs recorded from striatal neurons obtained from young WT ($n = 6$), mature WT ($n = 7$), and mature D2KO ($n = 7$) mice. Note that there are no significant differences between young WT and mature WT (unpaired t test, $P > 0.2$), or between mature WT and mature D2KO mice (unpaired t test, $P > 0.1$). (*B*) Comparison of the cumulative amplitude distributions of sEPSCs between young WT ($n = 5$, thin line) and mature WT mice ($n = 5$, thick line). There are 100 events in each line. Note that there is overlap of the amplitude distributions of sEPSCs from young WT and mature WT mice.

amplitudes obtained from different cells, we plotted the amplitude distribution curves from two comparison groups (young and mature WT mice) with equal number of events for each cell as shown in Fig. 4*B*. There is an overlap of the amplitude distributions of the young WT and mature WT mice. We observed similar overlap of the amplitude distributions when comparing all of the other age and treatment groups (data not shown). No significant age- or treatment-related differences in the amplitude, rise time (10–90%), or decay time constant of sEPSCs were observed in either species (Table 1).

There was no significant difference in postsynaptic input resistance of striatal neurons obtained from VEH-injected and 6-OHDA-injected mature rats, and no difference in input resistance was observed when comparing either the young and mature WT mouse groups, or when comparing the mature WT and mature D2KO groups (data not shown). There was a significant difference in postsynaptic input resistance when comparing young untreated (input resistance = 294.3 ± 12.8 MΩ, $n = 10$) and mature untreated (input resistance = 146.6 ± 13.5 MΩ, $n = 9$) rats (unpaired t test, $P < 0.05$). This developmental decrease in input resistance is in agreement with an earlier report (24). The lack of change in input resistance in most of the comparisons is not surprising because we measured this parameter in neurons filled with Cs^+ and QX-314, and changes in input resistance are likely to arise from differences in resting K^+ conductance.

Developmental Synaptic Depression Shares Mechanisms with Striatal LTD Induced by High-Frequency Afferent Activation. DA has been shown to be required for striatal LTD that can be induced by HFS in the white matter overlying striatum (15). We wanted to examine whether striatal LTD was inducible in 6-OHDA-injected rats and D2KO mice at the developmental period examined in our studies. Striatal LTD was induced in control slices from VEH-injected PD23–26 rats (EPSC amplitude = 64.3% ± 5.6% of pre-HFS control) and WT PD21–27 mice (EPSC amplitude = 46.6% ± 2.1% of pre-HFS control). An increase in PPR associated with LTD maintenance was also observed in slices from VEH-injected rats (PPR = 131.9% ± 7.5% of pre-HFS control, paired t test, $P < 0.01$, $n = 6$) and WT mice (PPR = 134.7% ± 7.8% of pre-HFS control, paired t test, $P < 0.01$, $n = 4$). However, striatal LTD could not be induced in slices from 6-OHDA-injected PD21–26 rats (EPSC amplitude = 93.3% ± 3.3% of pre-HFS control) and PD22–27 D2KO mice (EPSC amplitude = 94.6% ± 4.8% of pre-HFS control). No significant PPR change was observed after HFS application in slices from 6-OHDA-injected rats (PPR = 103.7% ± 6.6% of pre-HFS control, paired t test, $P > 0.8$, $n = 5$) and D2KO mice

Table 1. Comparison of the rise time (10–90%) and decay time constant (90–37%) (τ) of sEPSCs in different age and treatment groups

Animals	Age	Treatment	Rise time, ms	τ, ms
Rats	Young (PD12–14)	Untreated	2.10 ± 0.08	4.44 ± 0.47
	Mature (PD21–26)	Untreated	2.45 ± 0.23	4.40 ± 0.45
	Mature (PD23–26)	VEH	2.35 ± 0.19	4.03 ± 0.35
	Mature (PD22–26)	6-OHDA	2.60 ± 0.16	5.05 ± 0.42
Mice	Young (PD12–15)	WT	2.38 ± 0.12	4.38 ± 0.17
	Mature (PD21–26)	WT	2.07 ± 0.19	4.06 ± 0.17
	Mature (PD22–27)	D2KO	2.15 ± 0.16	3.85 ± 0.31

Note that there is no significant age- or treatment-related difference in rise time and τ (unpaired Student's t test).

(PPR = 103.4% ± 4.5% of pre-HFS control, paired t test, $P > 0.4$, $n = 7$). These data are consistent with the findings of other studies in mature rodent brain preparations (15, 25) and confirm the idea that DA and activation of D2 receptors are important for striatal LTD induction. These observations also reinforce the tight linkage between increased PPR and LTD expression as we reported earlier (18).

Discussion

DA-Dependent Developmental Decrease in Presynaptic Release Probability. We have obtained evidence that a decrease in probability of glutamate release occurs naturally in striatum, and that this form of plasticity is DA- and D2 receptor-dependent. The depression of transmission becomes apparent after PD20, and thus it is likely a consequence of a number of physiological changes that take place in the maturing striatum at about this time. Morphological and electrophysiological properties of striatal neurons have been reported to become mature after 3 postnatal weeks (24). Furthermore, the density of asymmetric axodendritic synapses, most of which are formed by glutamatergic afferents, increases to near adult levels by PD21 (26). Mature firing patterns of nigral DA neurons (27) and cortical neurons (28), and the occurrence of the depolarized "up-state" of striatal neurons (29), have been reported to appear within the same time window. Developmental studies (30–32) have shown that the arrival of dopaminergic axons to the striatum can be observed in the late embryonic stage, and dopaminergic innervation of the striatum continues to increase up to postnatal week 3. Cortical synapses undergo extensive maturation in the postnatal period, with the greatest increase in the density of asymmetrical synapses occurring between postnatal days 13 and 17 (33). These data suggest that the DA system that arises early in the ontogeny of the striatum has an organizing function in the development of this brain region.

Interestingly, the physiological changes taking place during this developmental time window are conducive to induction of striatal LTD in the slice preparation. High-frequency cortical input, depolarization of MSNs, and dopaminergic transmission are all required for LTD induction, and the morphological and physiological changes discussed would bring about all of these conditions. Thus, it is possible that the developmental decrease in release probability reflects an LTD-like process that is prominent during this stage of striatal maturation.

The DA and D2 receptor dependence of the developmental change in striatal transmission resembles the requirements for HFS-induced LTD, suggesting that these two forms of synaptic plasticity may be mechanistically related. This idea is also supported by the observation that HFS-induced LTD expression involves a decrease in the probability of neurotransmitter release, similar to that observed during postnatal development (18).

The developmental decrease in frequency of spontaneous neurotransmitter release is most likely another manifestation of the developmental decrease in probability of release. The developmental decrease in mEPSC frequency could be due to a decrease in the number of release sites or a loss of synapses. However, morphological studies indicate that the number of asymmetrical synapses actually increases during this developmental time window (26). Furthermore, the increase in PPR suggests that the depression of transmission is due to a decrease in probability of release rather than a decrease in number of release sites. Previous studies (34) have indicated that 6-OHDA lesions lead to a specific decrease in the dendritic spine density on MSNs. This would result in fewer asymmetrical synapses per neuron, and an accompanying decrease in the number of release sites. Thus, it is unlikely that the increase in mEPSC frequency we have observed in 6-OHDA-injected rats is due to an increase in the number of release sites.

Lack of Involvement of Postsynaptic Mechanisms. It is possible that changes in postsynaptic responsiveness or membrane properties could contribute to the alterations in sEPSC frequency that we have observed. However, our observation that sEPSC amplitude, rise time, and decay time constant do not change during development or across genotypes and treatment groups suggests that this is not the case. One would expect changes in sEPSC shape parameters if changes in dendritic filtering contributed to changes in event frequency.

Neuronal input resistance would not contribute to the changes in sEPSC frequency or PPR that we have observed, because we performed our experiments under voltage-clamp conditions. Furthermore, we filled neurons with Cs^+ and QX-314 to minimize any influence of resting K^+ conductances on the measurement of synaptic responses. It is noteworthy that a developmental change in striatal MSN input resistance has been observed in previous studies (24). This alteration in a key postsynaptic membrane property would most likely produce differences in MSN integration of synaptic responses at different stages in development. Thus, the overall developmental change in MSN responses to glutamatergic synaptic input is likely to involve a combination of changes in postsynaptic membrane properties and the presynaptic change that we have documented in the present study.

Involvement of Mechanisms Downstream from Presynaptic Neuronal Firing. The sEPSCs observed in striatal MSNs are TTX independent and appear to be mEPSCs (Fig. 3) (22). The finding that sEPSC frequency decreases during development indicates that the developmental decrease in presynaptic function involves mechanisms downstream from presynaptic neuronal activation. It is also possible that this presynaptic inhibition involves mechanisms downstream from calcium entry into presynaptic terminals (e.g., changes in the vesicle fusion/release process itself). This would constitute a novel mechanism for synapse development. However, inferences about the mechanisms underlying the developmental decrease in sEPSC frequency must be made with some caution. A recent study (35) has shown that inhibition of excitatory transmission by D2-like receptors is calcium dependent in the ventral tegmental area. Thus, it is possible that calcium-dependent mechanisms may contribute to dopaminergic modulation of glutamate release and could play a role in the developmental change in sEPSC frequency.

Previous reports described the appearance of spontaneous depolarizing postsynaptic potentials in striatal neurons after DA depletion in adult rats (36, 37). These increases may be due to a reversal of the DA-dependent regulatory process that we are describing in the present study. However, other mechanisms may also be involved in 6-OHDA-induced increase in spontaneous transmission in the adult rat. It should be noted that in these past studies no attempt was made to determine the mechanisms underlying the increased frequency of spontaneous depolarizing postsynaptic potentials. We have provided evidence that the increased spontaneous transmission after DA depletion is due to a loss of a form of presynaptic depression that is DA dependent.

Lack of Involvement of an Acute Effect of DA. The synaptic depression that we have characterized could be the result of a tonic effect of DA acting through presynaptic D2 receptors, reminiscent of the actions of adenosine and A1 receptors (38). However, the observation that acute application of DA receptor antagonists does not alter synaptic transmission, PPR, or sEPSC frequency indicates that there is not a tonic activation of DA receptors that can be relieved by acute antagonist application under normal conditions. Therefore, the persistence of high-efficacy transmission beyond PD20 that we have observed in 6-OHDA-injected rats and D2KO mice is likely because of the loss of organizational effects of DA and D2 receptors on the

development of striatal synapses and not to the absence of DA inhibitory tone on mature axons of cortical or thalamic glutamatergic neurons. This idea is also consistent with findings of past studies examining effects of acute DA receptor agonist application. Application of DA or D2 agonists does not consistently inhibit striatal transmission in brain slices from rats or mice unless the animals have been treated with neuroleptics (39). A few studies (40, 41) have suggested that acute DA application inhibits stimulus-evoked striatal synaptic transmission. However, these actions may well be because of postsynaptic effects of DA. Studies by Bargas and coworkers (42) suggest that D2 receptor activation can reduce the frequency of sEPSCs evoked by the K^+ channel blocker 4-aminopyridine, but these effects were observed in a small subpopulation of neurons. Thus, these effects are unlikely to account for the large increases in PPR and decreases in sEPSC frequency that we have observed in our studies. DA appears to inhibit transmission by an alternative mechanism that most likely involves initiation of processes involved in induction of an LTD-like process, with the ultimate result being depression of glutamate release. Our findings indicate that a major role for DA and D2 receptors in striatum is to limit the efficacy of striatal glutamatergic synaptic inputs to MSNs.

Implications for Striatum-Based Behaviors. The loss of the DA-dependent decrease in synaptic efficacy *in vivo* could lead to disturbances of striatal and basal ganglia function, and consequently produce changes in motor and cognitive function. Changes in motor function and learning have been observed in both neonatal 6-OHDA-treated rats and D2KO mice, although the phenotypes differ between these rodent models (43–48). Some of the alterations in striatum-based behaviors in these animal models could result, at least in part, from an absence of the synaptic changes that we have described. However, the exact role of these synaptic mechanisms in behavior will have to be elucidated in future studies. The fact that the neonatal 6-OHDA-injected rats have different phenotypes than the D2KO mice may be due to compensatory changes in response to a total loss of dopaminergic innervation at an early age that are more pronounced than those triggered by the loss of one receptor. It is also worth noting that there are a number of behaviors that have not been examined in both animal models, including striatum-based learning paradigms that could involve striatal synaptic plasticity. Thus, it will be of interest to compare behavioral changes in neonatal intrastriatal 6-OHDA rats and D2KO mice by using these learning paradigms.

The findings presented in this study strongly support the idea that a novel presynaptic mechanism producing decreased synaptic efficacy occurs naturally in a DA-dependent manner during development of striatal synapses *in vivo*. It will be interesting to determine the role of this form of plasticity in striatal functions such as motor sequencing and habit learning.

We thank Drs. A. Y. Deutch and M. Bubser for their support in immunocytochemical studies. Help with manuscript preparation was provided by Drs. S. Choi, J. M. Tepper, and R. W. Tsien. We also thank Dr. J. H. Moore for his suggestions on statistical analysis. This work was supported by National Institutes of Health Grant NS30470 and a grant from the Tourette Syndrome Association to D.M.L., and National Institutes of Health Grant DA12062 to D.K.G. and M.J.L. The B6.129S2-*Drd2*^{tm1Low} mice are available from the Induced Mutant Resource at The Jackson Laboratory.

1. Albin, R. L., Young, A. B. & Penney, J. B. (1989) *Trends Neurosci.* **12,** 366–375.
2. Jog, M. S., Kubota, Y., Connolly, C. I., Hillegaart, V. & Graybiel, A. M. (1999) *Science* **286,** 1745–1749.
3. Kemp, J. M. & Powell, T. P. (1970) *Brain* **93,** 525–546.
4. McGeorge, A. J. & Faull, R. L. (1989) *Neuroscience* **29,** 503–537.
5. Beckstead, R. M. (1984) *J. Comp. Neurol.* **223,** 313–346.
6. Bouyer, J. J., Park, D. H., Joh, T. H. & Pickel, V. M. (1984) *Brain Res.* **302,** 267–275.
7. Hattori, T., McGeer, E. G. & McGeer, P. L. (1979) *J. Comp. Neurol.* **185,** 347–353.
8. Freund, T. F., Powell, J. F. & Smith, A. D. (1984) *Neuroscience* **13,** 1189–1215.
9. Arbuthnott, G. W., Ingham, C. A. & Wickens, J. R. (1998) *Adv. Pharmacol.* **42,** 733–736.
10. Schultz, W. (1982) *Prog. Neurobiol.* **18,** 121–166.
11. DeLong, M. R. (1990) *Trends Neurosci.* **13,** 281–285.
12. Gerfen, C. R., Engber, T. M., Mahan, L. C., Susel, Z., Chase, T. N., Monsma, F. J., Jr., & Sibley, D. R. (1990) *Science* **250,** 1429–1432.
13. Surmeier, D. J. & Kitai, S. T. (1993) *Prog. Brain Res.* **99,** 309–324.
14. Aosaki, T., Graybiel, A. M. & Kimura, M. (1994) *Science* **265,** 412–415.
15. Calabresi, P., Maj, R., Pisani, A., Mercuri, N. B. & Bernardi, G. (1992) *J. Neurosci.* **12,** 4224–4233.
16. Bliss, T. V. & Collingridge, G. L. (1993) *Nature (London)* **361,** 31–39.
17. Choi, S. & Lovinger, D. M. (1997) *J. Neurosci.* **17,** 8613–8620.
18. Choi, S. & Lovinger, D. M. (1997) *Proc. Natl. Acad. Sci. USA* **94,** 2665–2670.
19. Kelly, M. A., Rubinstein, M., Asa, S. L., Zhang, G., Saez, C., Bunzow, J. R., Allen, R. G., Hnasko, R., Ben-Jonathan, N., Grandy, D. K. & Low, M. J. (1997) *Neuron* **19,** 103–113.
20. Debanne, D., Guerineau, N. C., Gahwiler, B. H. & Thompson, S. M. (1996) *J. Physiol. (London)* **491,** 163–176.
21. Katz, B. & Miledi, R. (1968) *J. Physiol. (London)* **195,** 481–492.
22. Tang, K. C. & Lovinger, D. M. (2000) *J. Neurophysiol.* **83,** 60–69.
23. Tyler, E. C. & Lovinger, D. M. (1995) *Neuropharmacology* **34,** 939–952.
24. Tepper, J. M. & Trent, F. (1993) *Prog. Brain Res.* **99,** 35–50.
25. Calabresi, P., Saiardi, A., Pisani, A., Baik, J. H., Centonze, D., Mercuri, N. B., Bernardi, G. & Borrelli, E. (1997) *J. Neurosci.* **17,** 4536–4544.
26. Sharpe, N. A. & Tepper, J. M. (1998) *Neuroscience* **84,** 1163–1175.
27. Tepper, J. M., Trent, F. & Nakamura, S. (1990) *Brain Res. Dev. Brain Res.* **54,** 21–33.
28. Kasper, E. M., Larkman, A. U., Lubke, J. & Blakemore, C. (1994) *J. Comp. Neurol.* **339,** 475–494.
29. Wilson, C. J. (1993) *Prog. Brain Res.* **99,** 277–297.
30. Voorn, P., Kalsbeek, A., Jorritsma-Byham, B. & Groenewegen, H. J. (1988) *Neuroscience* **25,** 857–887.
31. Specht, L. A., Pickel, V. M., Joh, T. H. & Reis, D. J. (1981) *J. Comp. Neurol.* **199,** 255–276.
32. Specht, L. A., Pickel, V. M., Joh, T. H. & Reis, D. J. (1981) *J. Comp. Neurol.* **199,** 233–253.
33. Hattori, T. & McGeer, P. L. (1973) *Exp. Neurol.* **38,** 70–79.
34. Ingham, C. A., Hood, S. H. & Arbuthnott, G. W. (1989) *Brain Res.* **503,** 334–338.
35. Koga, E. & Momiyama, T. (2000) *J. Physiol. (London)* **523,** 163–173.
36. Galarraga, E., Bargas, J., Martinez-Fong, D. & Aceves, J. (1987) *Neurosci. Lett.* **81,** 351–355.
37. Calabresi, P., Mercuri, N. B., Sancesario, G. & Bernardi, G. (1993) *Brain* **116,** 433–452.
38. Lovinger, D. M. & Choi, S. (1995) *Neurosci. Lett.* **199,** 9–12.
39. Calabresi, P., De Murtas, M., Mercuri, N. B. & Bernardi, G. (1992) *Ann. Neurol.* **31,** 366–373.
40. Cepeda, C., Colwell, C. S., Itri, J. N., Chandler, S. H. & Levine, M. S. (1998) *J. Neurophysiol.* **79,** 82–94.
41. Calabresi, P., Benedetti, M., Mercuri, N. B. & Bernardi, G. (1988) *Neuroscience* **27,** 145–157.
42. Flores-Hernandez, J., Galarraga, E. & Bargas, J. (1997) *Synapse* **25,** 185–195.
43. Breese, G. R., Smith, R. D. & Cooper, B. R. (1975) *Pharmacol. Biochem. Behav.* **3,** 1097–1106.
44. Shaywitz, B. A. & Pearson, D. A. (1978) *Pharmacol. Biochem. Behav.* **9,** 173–179.
45. Archer, T., Danysz, W., Fredriksson, A., Jonsson, G., Luthman, J., Sundstrom, E. & Teiling, A. (1988) *Pharmacol. Biochem. Behav.* **31,** 357–364.
46. Moy, S. S. (1995) *Pharmacol. Biochem. Behav.* **52,** 433–441.
47. Baik, J. H., Picetti, R., Saiardi, A., Thiriet, G., Dierich, A., Depaulis, A., Le Meur, M. & Borrelli, E. (1995) *Nature (London)* **377,** 424–428.
48. Kelly, M. A., Rubinstein, M., Phillips, T. J., Lessov, C. N., Burkhart-Kasch, S., Zhang, G., Bunzow, J. R., Fang, Y., Gerhardt, G. A., Grandy, D. K. & Low, M. J. (1998) *J. Neurosci.* **18,** 3470–3479.